

Bond switching from two- to three-dimensional polymers of C₆₀ at high pressureDam Hieu Chi,¹ Y. Iwasa,^{2,3} T. Takano,² T. Watanuki,⁴ Y. Ohishi,⁵ and S. Yamanaka⁶¹Faculty of Physics, Hanoi National University, 334 Nguyen Trai Str., Hanoi, Vietnam²Institute for Materials Research, Tohoku University, Sendai, 980-8577, Japan³CREST, Japan Science and Technology Corporation, Kawaguchi, 332-0012, Japan⁴Synchrotron Radiation Center, JAERI, Koto 1-1, Hyogo 679-5198, Japan⁵JASRI-SPring-8, Koto 1-1, Hyogo 679-5198, Japan⁶Department of Applied Chemistry, Hiroshima University, Kagamiyama, Higashi-Hiroshima, 739-8527, Japan

(Received 5 August 2003; published 20 October 2003)

In situ high pressure x-ray diffraction experiments revealed that a transformation from the two-dimensional (2D) tetragonal C₆₀ polymer to a three-dimensional (3D) polymer takes place via a highly anisotropic deformation of C₆₀ molecules along the *c* axis, as an irreversible first-order transformation above 20 GPa. In the 3D polymer phase, the 2+2 bonds remain in the 2D plane, while neighboring layers are connected by the 3+3 bonds. The bulk modulus of the 3D polymer was 407 GPa, being slightly smaller than that of diamond.

DOI: 10.1103/PhysRevB.68.153402

PACS number(s): 61.48.+c, 61.50.Ah, 61.50.Ks

Carbon based nanostructures are attracting a great deal of attention in this decade, because of their vast variety and associated functionalities. Among them, C₆₀ based nanostructures, so called fullerene polymers, have provided unique opportunities in terms of rich structures and properties.^{1,2} Simultaneous application of high pressure and high temperature to C₆₀ monomer solids has been a powerful tool to search for crystalline forms of novel nanonetwork structures.³ One or two-dimensional polymers, which were synthesized by this method, have crosslinked C₆₀ connected by 2+2 cycloaddition.⁴ Soon later, 3D polymerization was found to occur by two groups which showed that hardness of 3D polymers is comparable to or even larger than that of diamond.^{5,6} Since then, researchers have shown that the application of high pressure and temperature to C₆₀ produces various kinds of 3D polymers. However, detailed structures, physical properties, and polymerization mechanisms of 3D polymers need more investigations.

In 1999, a different approach was proposed by Okada and co-workers, who predicted a pressure-induced phase transformation of the preformed 2D C₆₀ to 3D polymers, based on a first principle local density approximation (LDA) calculation.⁷ This route is quite unique, since it is free from orientational disorder, which is inevitable in the conventional high-pressure–high-temperature treatment of monomer solid. In the mean time, Meletov *et al.* found an occurrence of irreversible phase transformation above 20 GPa, by a high-pressure Raman experiment on the tetragonal (T-) C₆₀ polymer, being strongly indicative of 3D polymerization.⁸ Here, we report a structural study on T-C₆₀ polymer under high pressure up to 37 GPa. We found that C₆₀ exhibits a pancake-type deformation, followed by a transition at about 24 GPa associated with a formation of interlayer 3+3 cycloaddition along the body diagonal. The structural model obtained differs from the theoretical prediction.⁷ The bulk modulus of the high-pressure 3D polymer phase was determined as 407 GPa, which is slightly smaller than that of diamond (443 GPa).

Synthesis of 2D polymer single crystals was established in 2002.^{9–11} Single crystals of T-C₆₀ polymer, grown accord-

ing to Ref. 10, were ground into powders and subjected to an *in situ* high-pressure x-ray diffraction experiment at room temperature. High pressure was generated with a diamond anvil cell (DAC) equipped with an inconel gasket. Powder samples of T-C₆₀ polymer were loaded with a Ruby chip in a hole made in the gasket. Two experiments with different pressure medium (helium and methanol/ethanol mixture with pressure solidification point of 12 GPa and 10.8 GPa, respectively) were carried out in parallel. Pressure was determined by the Ruby-fluorescence method. X-ray diffraction experiments were carried out on the beamline BL10XU at the synchrotron radiation facility, SPring-8, Japan. Incident x-ray was monochromatized at 0.618817(3) Å with a Si double crystal and collimated to 0.1 mm in diameter. An imaging plate was used for detecting the diffraction patterns. Structure analysis was carried out using the GSAS²¹ and Cerius2 software.

Figure 1 shows the powder x-ray diffractograms of T-C₆₀ polymers at various pressures, recorded using the Helium pressure medium. For T-polymer single crystals, two kinds of stacking patterns of 2D C₆₀ polymer planes are reported

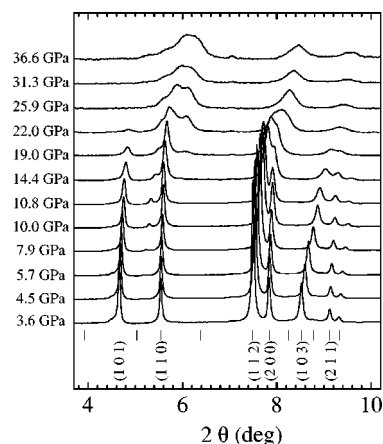


FIG. 1. Synchrotron x-ray diffraction patterns of T-C₆₀ polymers at high pressure with He pressure medium. Wavelength was $\lambda = 0.618817(3)$ Å. Background was subtracted from the raw data.

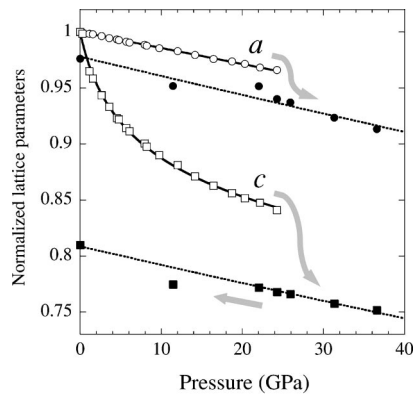


FIG. 2. Pressure dependence of lattice parameters a (circles) and c (squares) of T-C₆₀ polymers, normalized by the ambient pressure values of $a=9.081$ Å and $c=15.076$ Å. Open circles and squares show plots for 2D polymers, while filled circles and squares represent for 3D polymers. Filled circles and squares at 11 GPa and 0.1 MPa are taken from the data in the pressure-releasing process.

with different space groups: Chen/Yamanaka¹⁰ and Narymbetov *et al.*¹¹ claimed $Immm$ and $P42/mmc$, respectively. The crystal used in this study was synthesized by the former method, and the $Immm$ space group was confirmed by a single-crystal analysis. Though $Immm$ is the space group for the orthorhombic structure, we assumed $a=b$ because these two values are too close to distinguish, particularly at high pressure. Most of the peaks at ambient pressure were successfully indexed on the pseudotetragonal cell $a=9.081$ Å and $c=15.076$ Å, in a consistent manner with the previous paper.¹⁰ However, we observed (210) and (104) peaks, which are forbidden in $Immm$ but allowed in $P42/mmc$. A Rietveld analysis shown in Fig. 3(a) indicates that 20% of $P42/mmc$ phase is included in the powder sample. The pressure-induced peak shift was strongly dependent on reflection indices, being indicative of highly anisotropic compression. Above 20 GPa, we found a dramatic change in the diffraction pattern.

Figure 2 displays the pressure dependence of lattice parameters for T-C₆₀ polymer, which are normalized by the ambient pressure values. In addition to the change in the diffraction pattern above 20 GPa (Fig. 1), the lattice parameters display discontinuous jumps, associated with a coexistence region of the two phases between 21 and 24 GPa. The high-pressure state was retained in the pressure release process. The parallel experiments with He and methanol/ethanol pressure media showed an essentially identical behavior.

Up to 25 GPa, the contraction was fairly anisotropic, being consistent with the character of 2D polymer structure. The pressure dependence of the c parameter was well fitted to the modified second-order Murnaghan equation-of-state (EOS).¹²

$$P = (K_c/K'_c)[(c_0/c)^{K'_c} - 1],$$

where $1/K_c$ is the compressibility of c parameter at atmospheric pressure, K'_c is its pressure derivative (dK_c/dP), and c_0 is the c value at ambient pressure.¹³ The a parameter, on the other hand, was fitted by the linear relation up to 20

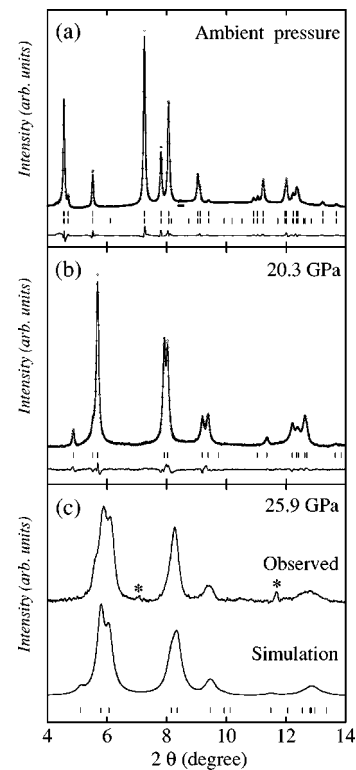


FIG. 3. (a) Top: experimental points and the best Rietveld fit pattern for the 2D polymer phase at ambient pressure. Middle: Ticks showing the 2θ positions for the allowed reflections of the $Immm$ and $P42/mmc$ phases. Bottom: Difference between the experiment and the fit. (b) Top: experimental points recorded at $P=20$ GPa and the best Rietveld fit pattern for the compressed 2D polymer phase. Middle: Ticks showing the 2θ positions. Bottom: Difference between the experiment and the fit. (c) Experimental data at $P=26$ GPa and simulated patterns based on the structural model in Fig. 4(c). Peaks marked by asterisks are not from samples.

GPa. The ambient pressure compressibility was determined as 0.001 43 and 0.0343 GPa⁻¹ for a and c axes, respectively. The compressibility $1/K_c = d \ln c / dP$ is comparable to that for the fcc C₆₀ (Ref. 14), while the $d \ln a / dP$ is more than one order of magnitude smaller than $d \ln c / dP$, indicating that the 2+2 bond between C₆₀ is considerably strong. The anisotropic compressibility is qualitatively consistent with the recent papers published independently.^{14,15} More importantly, such anisotropy is close to the uniaxial compression, where a theoretical prediction of 3D polymer formation was made.⁷

The high-pressure state was maintained after releasing the pressure. The lattice parameters at $P=0.1$ MPa were $a=8.88$ Å and $c=12.1$ Å. Particularly the c parameter shows a significant contraction in comparison to that of the starting T phase. Also, the anisotropy parameter $\sqrt{2}a/c$ of the quenched high-pressure phase was 1.04, while $\sqrt{2}a/c$ was 0.852 for the starting 2D-T polymer at ambient pressure. This means that the interball distance within the 2D layer is larger than that between the neighboring layers in the high-pressure state, indicating an occurrence of 3D polymerization. The pressure dependence of the 3D polymer phase is

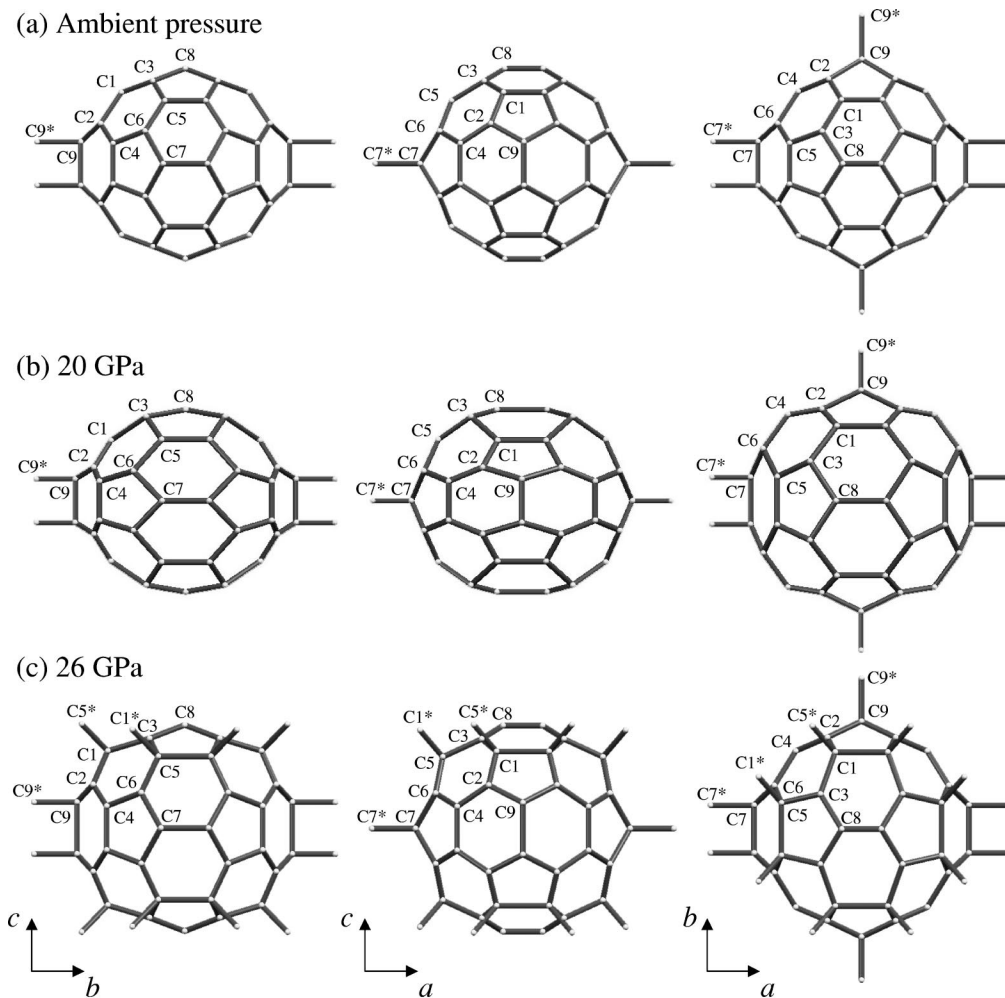


FIG. 4. Structural models for the 2D polymer at ambient pressure, (a) at $P=20$ GPa (b), and for the 3D polymers at $P=26$ GPa. (c) The models (a) and (b) were obtained from the Rietveld analysis in Figs. 3(a) and (b) respectively, while the model (c) corresponds to the simulation of the diffraction pattern in Fig. 3(c).

very isotropic and the bulk modulus was found to be 407 GPa, being slightly smaller than that of diamond (443 GPa).

To obtain an insight into the mechanism of bond switching from 2D to 3D polymer structures, determination of the crystal structure before and after the transition is crucial. First, we have carried out a Rietveld analysis on the data taken at $P=20$ GPa. The number of the observed peaks was only 17. Thus, we put additional constraints so as to maintain the cage-like structure. This allowed us to reduce the number of independent parameters to ten, and we succeeded in a stable refinement. Figure 3(b) shows the observed and best Rietveld-fit patterns at 20 GPa, and Fig. 4(b) displays a model structure determined by this refinement. The results of the refinement together with the coordinates are given in Ref. 17.

As shown in Fig. 4(a), C_{60} molecules in the T polymer at ambient pressure looks rather spherical, despite the formation of the intermolecular 2+2 bonds in the ab plane. In sharp contrast, C_{60} molecules at 20 GPa are significantly distorted by compression. Such a pancake-type deformation was essential to explain the intensity ratios between (110) and (112) or between (200) and (112). Similar deformation

just before the bond formation between C_{60} molecules has been pointed out by a tight-binding calculation for the case of dimerization process,¹⁸ and ascribed to the antibonding nature of the wavefunction of neighboring C_{60} molecules. The present result provides the first experimental evidence for this type of deformation before the occurrence of bond switching.

For the case of the 3D polymer phase at 26 GPa, the gross broadening and small number of resolved peaks did not allow us a reliable Rietveld refinement. Thus a structural model was constructed based on the geometrical consideration within the $Immm$ space group. In the present case, the intermolecular bonds in the 2D plane starts from the 2+2 cycloaddition, and thus it is very likely that the intralayer 2+2 bonds are maintained in the 3D polymer phase. Also, as displayed in Fig. 2, the pressure dependences of a parameters for 2D and 3D polymer phases are almost parallel to each other, strongly indicating that the bonding nature in the 2D plane is identical. Hence, we assumed the network of 2+2 cycloaddition in the ab plane for the 3D polymer phase.

As an interlayer bond, Okada and co-workers⁷ predicted a model in which C_{60} molecules are connected *via* a [0,0]

cyclophane-type bonding, namely C2-C5* and C5-C2*. Indexation of carbon atoms is given in Fig. 4. In their uniaxially compressed structure with cell parameters of $a = 9.09 \text{ \AA}$ and $c = 10.70 \text{ \AA}$, this type of bonding was stable. In the present experiment, however, the cell parameters are $a = 8.53 \text{ \AA}$ and $c = 11.6 \text{ \AA}$ at 26 GPa, or $a = 8.88 \text{ \AA}$ and $c = 12.1 \text{ \AA}$ at ambient pressure. The c parameter is considerably larger than that in the hypothetical uniaxial pressurization, and thus the nearest C-C bonds are found in different combinations, C5-C1* and C1-C5*. Figure 3(c) shows the comparison of the experimental and simulated diffraction patterns. Fair agreement of intensity distribution without any fitting parameters indicates that this 3+3 cycloaddition is the most plausible model based on the present experiment. The coordinates in this model are also tabulated in Ref. 17.

The structural model for 26 GPa is shown in Fig. 4(c). This model for the 3D polymer is identical to that proposed for the one produced by a shear stress on fcc C₆₀.¹⁶ In contrast to the pancake-like distortion at 20 GPa, the molecule displays an outward deformation which was crucial to explain the intensity distribution of the diffraction data. Particularly, C1 and C5 protrude from cage-like structure and interconnect neighboring C₆₀ molecules.

The present observation confirmed that the transformation found by Raman measurement⁸ is indeed structural in nature. However, such a structural transition was not found in the previous structural study on T-polymers.¹⁴ A possible reason for this disagreement is the strong dependence of the pressure-induced polymerization of the T-polymer on the structural details. There are two kinds of T-C₆₀ polymer phases, which are characterized by space groups of *Immm* and *P42/mmc*. Since the starting 2D polymer in the present experiment is *Immm* with 20% impurity of *P42/mmc*, the 3D polymerization that is a characteristic of *Immm* did take place. However, in samples with *P42/mmc* space group as a

majority phase, a different transition is expected at different pressure, and it is a competing process with amorphization due to the nonhydrostaticity of pressure in DAC. This could be the reason for the observed amorphization in Ref. 14.

Finally, we compare the present results with other model of 3D polymer phase. Researchers have produced 3D polymers with tetragonal or pseudotetragonal unit cells, mainly by the conventional method, which is the application of high pressure at high temperature.^{19,20} A shear stress on fcc C₆₀ also produced tetragonal 3D polymers.¹⁶ The cell parameters of the so far reported (pseudo) tetragonal 3D polymers are very similar to the present result, $a = 8.88 \text{ \AA}$ and $c = 12.1 \text{ \AA}$ at ambient pressure. These results indicate that the 3D polymers with tetragonal structures are rather stable. For this structure, Chernozatonskii *et al.* proposed a model, in which the intermolecular bonds are formed along the body diagonal of the unit cell with the 3+3 cycloaddition, while the C₆₀ network in the ab plane is made of two types of bondings.²⁰ One is the 2+2 bonds along the a axis, and the other is the cyclobutane rings produced by the Stone-Wales transformation. On the other hand, Serebryanaya's model is identical to ours.¹⁶ These differences might indicate that 3+3 cycloaddition is a common structure, while the intralayer bonds depend on the synthesis procedure.

In summary, we first demonstrated a structural transition process from 2D to 3D polymer of C₆₀ by *in situ* high-pressure x-ray diffraction study. Under pressure, C₆₀ is deformed predominantly along the c axis, followed by a discontinuous formation of interlayer 3+3 cycloaddition. Such behavior should be common to pressure-induced polymerization processes for molecular materials.

Authors are indebted to T. Takenobu and M. Isshiki for their experimental assistance. They are grateful to S. Okada for stimulating discussions. This work has been partly supported by a Grant from the MEXT, Japan.

¹T.L. Makarova *et al.*, Nature (London) **413**, 716 (2001).

²B. Sundqvist, Adv. Phys. **48**, 1 (1999).

³Y. Iwasa *et al.*, Science **264**, 1570 (1994).

⁴M. Nunez-Regueiro *et al.*, Phys. Rev. Lett. **74**, 278 (1995).

⁵V.D. Blank *et al.*, Phys. Lett. A **188**, 281 (1994).

⁶V.V. Brashkin, A.G. Lyapin, and S.V. Popova, JETP Lett. **64**, 802 (1996).

⁷S. Okada, S. Saito, and A. Oshiyama, Phys. Rev. Lett. **83**, 1986 (1999).

⁸K.P. Meletov *et al.*, Chem. Phys. Lett. **341**, 435 (2001).

⁹X. Chen *et al.*, Chem. Phys. Lett. **356**, 291 (2002).

¹⁰X. Chen and S. Yamanaka, Chem. Phys. Lett. **360**, 501 (2002).

¹¹B. Narymbetov *et al.*, Chem. Phys. Lett. **367**, 157 (2003).

¹²F.D. Murnaghan, Proc. Natl. Acad. Sci. U.S.A. **30**, 244 (1947); J.R. Macdonald and D.R. Powell, J. Res. Natl. Bur. Stand., Sect. A **75**, 441 (1971).

¹³S.J. Duclos *et al.*, Nature (London) **351**, 380 (1991).

¹⁴J.M. Leger *et al.*, Solid State Commun. **121**, 241 (2002).

¹⁵S. Kawasaki *et al.*, Solid State Commun. **125**, 637 (2003).

¹⁶N.N. Serebryanaya *et al.*, Solid State Commun. **118**, 183 (2001).

¹⁷See EPAPS Document No. E-PRBMDO-68-083339 for the results of the Rietveld refinement and coordinates for ambient pressure, 20 GPa and 26 GPa. A direct link to this document may be found in the online article's HTML reference section. The document may also be reached via the EPAPS homepage (<http://www.aip.org/pubservs/epaps.html>) or from <ftp.aip.org> in the directory /epaps/. See the EPAPS homepage for more information.

¹⁸T. Ozaki, Y. Iwasa, and T. Mitani, Chem. Phys. Lett. **285**, 289 (1998).

¹⁹L. Marques *et al.*, Science **283**, 1720 (1999).

²⁰L.A. Chernozatonskii, N.R. Serebryanaya, and B.N. Mavrin, Chem. Phys. Lett. **316**, 199 (2000).

²¹A. C. Larson and R.B. von Dreele, General Structural Analysis System, Los Alamos National Laboratory, 1998.